Comparison of CryoSat-2 and ENVISAT radar freeboard over Arctic sea-ice: Toward an improved Envisat freeboard retrieval

Kevin Guerreiro[1], Sara Fleury[1], Elena Zakharova[1,2], Alexei Kouraev[1,2,3], Frédérique Rémy[1], and Philippe Maisongrande[1]

[1]Laboratoire d'Etudes en Géophysique et Océanographie Spatiales, Centre National de la Recherche Scientifique (LEGOS - CNRS, UMR5566), Université de Toulouse, 31400 Toulouse, France
[2]State Oceanography Institute, St. Petersburg Branch, St. Petersburg, Russia
[3]Tomsk State University, Tomsk, Russia

Correspondence to: Guerreiro Kevin, kevin.guerreiro@legos.obs-mip.fr

Abstract. During the past decade, sea-ice freeboard has been monitored with various satellite altimetric missions with the aim of producing long-term time series of ice thickness. While recent studies have demonstrated the capacity of the CryoSat-2 mission (2010-) to provide accurate freeboard measurements, the current estimates obtained with the Envisat mission (2002-2012) still require some large improvements.

To improve Envisat freeboard retrieval, we first compare CryoSat-2 and Envisat radar freboard estimates during the common flight period (2010/11 and 2011/12 sea-ice growth seasons). The along-track analysis shows that unlike for CryoSat-2, the sea level as retrieved by Envisat is systematically located above the level of sea-ice floes. Consequently, Envisat radar freeboard estimates display unrealistic negative values during the entire ice growth season and all over the circumpolar region. This result is attributed to the sensitivity of pulse-limited waveforms to ice surface properties (surface roughness and snow volume scattering) and to the use of a threshold retracker.

The analysis of the gridded radar freeboard difference together with the corresponding Envisat pulse peakiness maps suggests that the discrepancy between the two sensors is also related to the surface properties of sea-ice floes. This strong linkage is, here as well, attributed to the higher sensitivity of pulse-limited waveform echoes to the variability of ice surface properties (surface roughness and snow volume scattering) and to the use of a threshold retracker.

Based on the relation between the Envisat pulse-peakiness and the radar freeboard difference, we produce a monthly CryoSat-2-like version of Envisat freeboard (Envisat/PP). The Envisat/PP dataset displays a similar spatial distribution as CryoSat-2 (RMSD = 1.5 cm) during the two ice growth seasons and for all month of the period of study.

The comparison of the altimetric datasets with *in situ* ice draft measurements during the common flight period shows that the Envisat/PP dataset (RMSE = 12 - 28 cm) is as accurate as CryoSat-2 (RMSE = 15 - 21 cm) and highly more accurate than the uncorrected Envisat dataset (RMSE = 178 - 179 cm).

The comparison of the improved Envisat radar freeboard dataset is then extended to the rest of the Envisat mission to demonstrate the validity of PP-correction out of the calibration period. The good agreement between the Envisat/PP and the *in situ* ice draft dataset (RMSE = 13 - 32 cm) demonstrates the potential of the PP-correction to produce accurate freeboard estimates over the entire Envisat mission lifetime.

1 Introduction

Sea-ice is one of the most sensitive indicators of the Arctic climate system changes. Satellite observations have demonstrated that Arctic sea-ice extent has decreased at an average rate of 4% per decade from 1978 to 2010 and at an accelerated rate of 8.3% during the 1996-2010 period (Comiso, 2012). In addition to the sea-ice cover reduction, it has been shown that Arctic sea-ice is also thinning (Rothrock et al., 1999; Kwok and Rothrock, 2009). Based on submarine ice draft measurements, Rothrock et al. (1999) reported a decrease of ∼1.3 m in the 1990s relatively to ice thickness measurements obtained during the 1958-76 period. However, Holloway and Sou (2002) show that local submarine measurements can be impacted by large scale displacement of perennial ice and that sea-ice thickness should be monitored at a basin-scale to accurately estimate sea-ice volume changes.

Over the past decade, satellite radar altimeters have been used to estimate basin-scale sea-ice thickness. It is generally assumed that over snow-covered sea-ice, the main scattering horizon of the Ku-band (13.6 GHz) radar signal is located at the snow/ice interface (Beaven, 1995). Hence, Ku-band radar altimeters have been used to monitor the height of sea-ice above sea level, generally referenced as sea-ice freeboard. By assuming the hydrostatic equilibrium between the ocean and the snow-covered sea-ice, freeboard can be converted to ice thickness (Laxon et al., 2003). Following this methodology, sea-ice thickness has been estimated with the pulse-limited altimeters RA onboard ERS-1 and RA-2 onboard ERS-2 and Envisat (Laxon et al., 2003; Giles et al., 2008). While the Envisat ice thickness estimates are promising, the current prototype product (http://icdc.cen.uni-hamburg.de/1/projekte/esa-cci-sea-ice-ecv0.html) has a positive bias of 0.5 to 1.5 m and does not reproduce accurately the seasonal cycle of ice growth (Kern et al., 2015). It is the purpose of the European Space Agency (ESA) Sea Ice Climate Change Initiative project (SI-CCI) to improve RA-2 freeboard retrievals and to provide accurate time series of ice thickness over the Envisat mission lifetime (Ridout and Tonboe., 2012). More recently, sea-ice thickness was estimated with the Ku-band Synthetic Aperture Radar (SAR) Interferometric Radar Altimeter (SIRAL) onboard CryoSat-2. Unlike for Envisat, CryoSat-2 ice thickness estimates are in good agreement with *in situ* measurements and display a realistic seasonal cycle (Laxon et al., 2013; Kwok and Cunningham, 2015; Tilling et al., 2015).

The higher accuracy of Cryosat-2 ice thickness estimates as compared to Envisat ones rise an important question: Why does CryoSat-2 provide better estimates of ice thickness than Envisat while both sensors operate at the same central frequency? First of all, the bias in Envisat ice thickness estimates could be caused by an inaccurate conversion of freeboard to ice thickness. Having said that, the study by Kern et al. (2015) shows that even when using a similar parametrization of snow depth and ice density as in CryoSat-2 studies (Laxon et al., 2013; Kwok and Cunningham, 2015), the Envisat ice thickness estimates remain relatively inaccurate. In particular, the authors do not succeed to reproduce the seasonal ice growth cycle. This result suggests therefore that the bias in Envisat ice thickness estimates is driven by a bias in the freeboard fields rather than by an inaccurate conversion of freeboard to ice thickness.

The common flight period of Envisat and CryoSat-2 (November 2010-March 2012) represents an unique opportunity to analyse the bias in the Envisat freeboard fields. In Schwegmann et al. (2015), Envisat and CryoSat-2 radar freeboard datasets are compared over Antarctic sea-ice. While the spatial and temporal distributions are consistent, it is shown that CryoSat-2 radar

freeboard is thicker (thinner) for thick (thin) freeboard values. The authors conclude that the discrepancy between the two datasets is likely related with the difference of footprint characteristics between pulse-limited and SAR altimetry.

Over sea-ice, conventional pulse-limited altimeters such as Envisat have a typical footprint of 2-10 km (Connor et al., 2009). Unlike pulse-limited altimetry, the SAR technology and the Doppler post-processing allow to identify the along-track position of each scatterers and offer SIRAL an along-track footprint of $\sim$ 300 m (the across-track being unchanged). The reduction of the footprint size of the SAR mode has mainly 2 consequences on the monitoring of sea-ice. First of all, it allows to minimize the impact of bright-off reflections in the along-track direction and thus, improves the range estimation over ice floes. In addition, the Doppler post processing allows to sharpen the surface response of the radar signal, which reduces the impact of surface roughness and snow volume scattering on the retrieval of the altimetric range (Raney, 1995).

It is therefore very likely that the better results obtained with CryoSat-2 over sea-ice are related to the reduced impact of off-Nadir reflections and diffuse scattering effects on the radar signal. Following this theoretical basis, we seek to analyse the discrepancy of radar freeboard between CryoSat-2 and Envisat and its link with the ice surface properties. In particular, we seek to analyse the impact of surface specularity on the freeboard retrieval.

In section 2, we introduce the datasets used in the present study as well as the freeboard retrieval algorithms. Then, we compare CryoSat-2 and Envisat waveform echoes (section 3.1), along-track freeboard estimates (section 3.2) and gridded freeboard estimates (section 3.3). In section 3.4, we build a Cryosat-2-like version of Envisat freeboard based on the relation between the freeboard discrepancy between Envisat and CryoSat-2 and the Envisat pulse-peakiness. Finally, in section 3.5, we convert CryoSat-2, Envisat and the corrected Envisat freeboard datasets to ice draft fields and compare each dataset to *in situ* measurements.

2 Data and methodology

2.1 Envisat

Envisat was launched in 2002 by ESA and was set on the same orbit as the ERS-1/2 satellites, providing coverage of the Arctic Ocean up to 81.5°N. The RA-2 altimeter onboard Envisat includes a Ku-band pulse-limited radar altimeter with a bandwidth of 320 MHz. To derive the Envisat freeboard fields, we use the Sensor Geophysical Data Record (SGDR) product from ESA (http://www.aviso.altimetry.fr/) that is converted to NetCDF files by the Center of Topography of Oceans and Hydrosphere (CTOH). The netcdfs contain geolocated 20 Hz waveform echoes, orbit parameters, atmosphere corrections, mean sea surface correction (DTU15, Andersen and Knudsen (2015)) and tide corrections (FES14, Carrere et al. (2015)). Envisat freeboard is estimated from November 2010 to April 2011 for the first common winter and from November 2012 to March 2012 for the second common winter season. The reduced period during winter 2011/2012 is due to the end of the Envisat mission at the beginning of April 2012.

2.2 CryoSat-2

CryoSat-2 was launched by ESA in 2010 and was primarily designed for the observation of ice over land and ocean surfaces (Wingham et al., 2006). Although the highly inclined orbit of CryoSat-2 allows the monitoring of sea-ice freeboard up to 88°N, we only make use of observations bellow 81.5°N in the present study (maximum latitude of Envisat orbit). Bellow this latitude and over the Arctic ocean, CryoSat-2 operates mostly in SAR mode except for observations close to the coastline and for a narrow patch located between 130°W and 150°W and at north of 80°N where it is set in SAR Interferometry mode. As the purpose of the present study is to analyse the difference of radar freeboard between pulse-limited and SAR altimetry, we only consider freeboard observations in SAR regions and discard observations in SARIn regions for both CryoSat-2 and Envisat. The SIRAL altimeter onboard CryoSat-2 operates at the same central frequency (Ku-band) and with the same bandwidth (320 MHz) as Envisat.

In the present study, we produce freeboard fields from the CryoSat-2 Baseline-C l1b product that is also converted to NetCDF files by CTOH. The netcdfs contain geolocated 20 Hz waveform echoes, orbit parameters, atmosphere corrections, mean sea surface correction (DTU15, Andersen and Knudsen (2015)) and tide corrections (FES14, Carrere et al. (2015)). The atmospheric and oceanic corrections are identical for the Envisat and CryoSat-2 products. As for Envisat, CryoSat-2 freeboard is estimated from November 2010 to April 2011 for the first common winter and from November 2012 to March 2012 for the second common winter season.

2.3 Ancillary data

Daily sea-ice extent and MYI age fields are available at a 12.5 km resolution from NSIDC and are derived from AMSR-E and SSMIS passive microwave observations (Anderson and Tschudi, 2014).

The Beaufort Gyre Exploration Project (BGEP) moorings provide high frequency (0.5 Hz) measurements of sea-ice draft since August 2003 thanks to a network of 2 to 4 moorings located in the Beaufort Sea (http://www.whoi.edu). The buoys are equipped among other instruments of an Upward Looking Sonar (ULS) that measures the distance from the mooring to the bottom of the ice with a 420 kHz beam sonar. Sea-ice draft is then estimated by removing the depth of the mooring that is deduced from pressure measured every 40 seconds. The accuracy of each 0.5 Hz measurements is of ± 5 cm.

To provide simultaneous analysis of ice type with radar observations, we use Landsat-7 and Landsat-8 optical imagery. The georeferenced "natural color" images distributed by the USGS (http://earthexplorer.usgs.gov/) are obtained from a combination of visible (bands 6,5,4) and thermal (band 10) images and have a general resolution of 30 m. Due to a technical issues of the Landsat-7 imager, there are no usable image during the common flight period of CryoSat-2 and Envisat. We therefore use images out of the common flight period.

The Landsat-7 image used to collocate Envisat observations was acquired on the 16th April 2004 in the Beaufort Sea and the Landsat-8 image used to collocate CryoSat-2 observations was acquired on the 1st May 2015 in the Beaufort sea as well. In

both examples used in the present study, the time latency between the Landsat images and the altimetric observations is shorter than 24h in order to minimize the impact of sea-ice drift on the correlation between both datasets.

2.4 Freeboard retrievals

In this section we describe the methodology that is applied to CryoSat-2 and Envisat to derive radar freeboard. While the different measurement mode (pulse-limited and SAR) are expected to drive differences in the radar freeboard estimates, we try to keep the retrieval algorithms as similar as possible between the two sensors in order to reduce the impact of the processing chain on each dataset.

The procedure we apply to retrieve Envisat and CryoSat-2 radar freeboard is described in details in the ESA SI-CCI project (Ridout and Tonboe., 2012) and is based on the already published method used for ERS-2 (Peacock and Laxon, 2004; Laxon et al., 2003).

Radar freeboard is obtained by measuring the difference of range between the ocean and sea-ice floes. The discrimination between sea-ice and ocean observations is performed through the analysis of the radar waveform shape. Radar echoes over open water in sea-ice fractures (leads) are generally highly specular due to the presence of a thin and smooth layer of ice and/or of a flat ocean surface. On the opposite, radar returns over sea-ice floes are relatively diffuse due to the impact of sea-ice deformation and snow accumulation. Consequently, the discrimination between leads and ice floes can be performed with the analysis of the pulse peakiness (PP). In the present study, the PP is defined as follows :

$$PP = \frac{max(WF)}{\sum_{i=0}^{i=N_{WF}}(WF_i)} \tag{1}$$

Where WF represents the echo and N_{WF} is the number of range bins.

To distinguish lead from ice floe observations, the common methodology consists to use thresholds on the PP (Peacock and Laxon, 2004). In order to determine the appropriate thresholds, we collocate Landsat images with Envisat and CryoSat-2 PP observations as explained in the previous section. In Fig. 1, we show typical on-track Envisat (left) and CryoSat-2 (right) PP observations plotted over Landsat images.

The collocated analysis displays similar results for both Envisat and CryoSat-2. Over sea-ice leads, the PP is always higher than 0.3 and can reach 0.6 (not visible due to the colorbar saturation). Based on this result and other similar visual observations we define leads as observations with a PP higher than 0.3.

In most freeboard retrievals, a threshold on the PP is also applied to identify mixed echoes found in the neighbouring of sea-ice leads (see Fig. 1) and to only keep unambiguous ice floe observations (Laxon et al., 2003; Peacock and Laxon, 2004; Giles et al., 2008; Ricker et al., 2014). Based on visual observations of collocated Landasat images with PP values such as the one shown in Fig. 1, we define sea-ice floes as observations with a PP lower than 0.10.

To estimate the surface elevation of ocean and sea-ice floes from the waveform echoes, several methodologies are used in the literature. In the ESA SI-CCI project, two different retracker algorithms are employed to take into account the difference of the waveform shape over specular leads and diffuse ice floes (Ridout and Tonboe., 2012) wile in Ricker et al. (2014), the authors

use a single retracker for leads and ice floe observations. Following the latter study, we only use a single retracker and make no extra-correction. This choice is made to limit the potential bias driven by the use of different algorithms and to fully understand the discrepancies between Envisat and CryoSat-2 radar freeboard measurements. Having said that, the difference of waveform shape between the two radar altimeters is likely to drive a difference in the radar freeboard fields.

5   Over surfaces with an heterogeneous reflectivity such as sea-ice, basic retracking algorithms based on the waveform maximum power can be easily biased by off-nadir reflexions. For this reason, we use the more robust Threshold First-Maximum Retracker Algorithm (TFMRA) to estimate the surface level position (Helm et al., 2014). For both Envisat and CryoSat-2 and for both leads and ice floes observations, the TFMRA retracker is parametrized similarly: waveform echoes are first oversampled by a factor 10. Then, the first waveform echo maximum is identified by calculating the first derivative of the power echo using a

10   3-point Lagrangian and finally, the echo position is estimated at 50% of the first waveform echo maximum.
The next step of freeboard retrieval consists to interpolate the sea level underneath sea-ice floes and to estimate the height of ice floes above the interpolated sea level. As the sea level interpolation can drive large errors due to uncertainties in estimates of ocean tide, barometer tide and mean sea surface height, we argue that the sea level should only be interpolated within sections of 25 km around each lead. Once the sea level is interpolated, single freeboard measurements are calculated an smoothed

15   along the altimeter track with a 25 km window median. Finally, monthly freeboard observations are gridded onto a 12.5 km × 12.5 km polar stereographic grid using a median filter with a radius of 100 km. Similarly to the freeboard maps, the Envisat along-track PP is also converted to monthly gridded maps.

2.5   Freeboard-to-thickness conversion

To convert the freeboard (fb) height to Sea-Ice Thickness (SIT), we assume the hydrostatic equilibrium between the snow-

20   covered sea-ice and the ocean and we use the following expression:

$$SIT = \frac{h_s \rho_s + fb \rho_i}{\rho_w - \rho_i} \qquad (2)$$

where, h_s represents snow depth, ρ_i is ice density, ρ_s is snow density and ρ_w is sea water density.

To operate the freeboard-to-thickness conversion, several snow depth dataset have been employed. For instance, Laxon et al. (2003) and Giles et al. (2008) use the time and space-varying snow depth climatology (hereafter W99) from the study

25   by Warren et al. (1999). However, recent *in situ* observations have demonstrated that snow depth has thinned by 50% over First Year Ice relatively to the W99 climatology (Kurtz et al., 2013; Guerreiro et al., 2016). Following this result, Kwok and Cunningham (2015) estimate snow depth according to the following equation:

$$h_s(X, t, f_{MY}) = h_s^{W99}(X, t) f_{MY} + 0.5 h_s^{W99}(X, t)(1 - f_{MY}) \qquad (3)$$

where $h_s(X, t, f_{MY})$ represents the time (t) and space (X)-varying W99 climatology and f_{MY} is the Multi Year Ice (MYI)

30   fraction that they derive from the Advanced Scatterometer (ASCAT) following the study by Kwok (2004). In the present study,

we use a similar methodology to estimate snow depth except that we use a different dataset to derive MYI ratio. Indeed, the methodology based on ASCAT observations assumes a direct link between ice age and ice roughness, which is not necessarily true in any case. To overcome this issue, we use the National Snow and Ice Data Center (NSIDC) ice age dataset (http://nsidc.org/data/docs/daac/nsidc0611-sea-ice-age/, Anderson and Tschudi (2014)). In this product version, the ice age is calculated by tracking the ice through the comparison of adjacent passive microwave images as well as using wind forcing and buoys displacement information. In addition to not make the assumption of a constant correlation between ice age and ice roughness, this product has the advantage to be available during the entire Envisat mission (2002-2012). In the present study, monthly snow depth fields are therefore derived as follows: First, each ice pixel with ice older than 1 year is considered as MYI and pixels with ice younger than 1 year is considered as FYI. Then, we apply an average filter with a radius of 100 km (similarly to the freeboard datasets) and estimate the ratio of MYI observation within the filtering area to build MYI concentration maps. Finally, we use the resulting MYI ratio fields, the W99 climatology and Eq. 3 to determine monthly snow depth fields.

Based on the results by Alexandrov et al. (2010), recent studies attribute a lower density to MYI (882 $kg.m^{-3}$) than to FYI (917 $kg.m^{-3}$). To account for the difference of ice density between MYI and FYI, we use the same definition for ice density as in Kwok and Cunningham (2015):

$$\rho_i(f_{MY}) = \rho_i^{MY} f_{MY} + \rho_i^{FY}(1 - f_{MY}) \tag{4}$$

Where ρ_i^{MY} and ρ_i^{FY} are respectively set to 882 and 917 $kg.m^{-3}$ and where f_{MY} is the MYI concentration derived from the NSIDC MYI age dataset.

Regarding snow and sea water densities, we use the same parametrization as in Kwok and Cunningham (2015). More precisely, the snow density follows the monthly average prescribed by Warren et al. (1999) and the sea water density is set to 1024 $kg.m^{-3}$.

Another important step for the freeboard-to-thickness conversion is the correction of the slower wave propagation effect in the snow pack. Indeed, the radar signal propagates slower in snow than in the atmosphere, which drives an underestimation of the freeboard estimates. To correct this bias, we add the factor α (see Eq. 5) to correct the freeboard measurements as operated in Kwok and Cunningham (2015).

$$\alpha = h_s(1 + 0.5\rho_s)^{-1.5} \tag{5}$$

3 Results

3.1 Comparison of CryoSat-2 and Envisat waveform echoes

As a first analysis, we compare mean CryoSat-2 and Envisat waveforms echoes for observations originating from leads, MYI and FYI. Leads and ice floes are identified as described in section 2.4 and MYI and FYI observations are distinguished with

the NSIDC ice age dataset. More specifically, ice floes echoes located in areas with more than 70% of MYI are classified as MYI and ice floes located in areas with less than 30% are classified as FYI.

To average CryoSat-2 and Envisat waveform echoes, we use the same methodology as in the study by Zygmuntowska et al. (2013). Shortly, all waveform echoes are normalized and shifted so their maximum power is located in the same sampling bin (the 67th bin here). Then, all waveform echoes are averaged to produce a mean echo. To produce average echoes, we use all waveforms available during the November 2010 - April 2011 period and in the common under-flight area. Results are presented in Fig. 2

First of all, CryoSat-2 waveforms clearly displays a narrower Leading Edge Width (LEW) than Envisat waveforms. This difference is mostly caused by the smaller SAR footprint (Raney, 1995).

For both sensors, the difference of ice surface type tends to modify the shape of the leading edge. In particular, the LEW is much wider for MYI and FYI than for lead observations. This phenomenon is generally attributed to an increase of surface roughness and/or of volume scattering. As suggested by Fig. 2, the LEW widening displayed by MYI waveforms is larger for Envisat than for CryoSat-2 waveforms. Considering that MYI is generally rougher and covered by a thicker snow layer than FYI, this result suggests that SAR waveforms are less sensitive to the variations of surface properties than pulse-limited waveforms.

The lower sensitivity of CryoSat-2 waveforms to surface properties is mostly due to the the Doppler post-processing that allows to reduce the widening of the effective footprint related to the increase of surface roughness and/or volume scattering (Chelton et al., 2001; Raney, 1995).

The deformation of waveform echoes related to changes of surface properties is likely to drive biases on the altimetric range retrieval. This is particularly true when using empirical threshold retrackers that do not take into account the modification of the waveform shape (Kurtz et al., 2014). Considering the seemingly lower impact of ice surface properties on CryoSat-2 waveform echoes, our results suggest that CryoSat-2 ranges estimates should be less impacted by surface roughness and/or snow volume scattering changes. Hence, the better freeboard estimates obtained with CryoSat-2 are likely related to a lower sensitivity of waveform echoes to the variability of ice surface properties.

3.2 Comparison of along-track radar freeboard estimates

As CryoSat-2 and Envisat have a different orbit configuration, it is unfortunately not possible to compare the radar freeboard over the exact same track. Thus, all one can do is to compare the radar freeboard within the same Arctic region. In Fig. 3, we show ground tracks of Envisat and CryoSat-2 missions used to analyse typical along-track freeboard estimates. Both tracks are located in the in the Western part of the Arctic Ocean and were acquired on the 24th of February 2011. The ice type classification (grey tons) shows that both MYI and FYI observations are found bellow each track.

Figures 3-b and 3-c show the elevation of floes (grey) and leads (black) respectively for each satellite mission. The first striking difference between the 2 datasets is the dispersion of surface elevation. Over sea-ice leads, CryoSat-2 displays a relatively low standard deviation of surface elevation (4.2 cm) when compared to Envisat (7.8 cm). This result clearly demonstrates that CryoSat-2 provides more consistent sea level estimates than Envisat. The standard deviation of the floes surface elevation is

also lower for CryoSat-2 (8.6 cm) than for Envisat (18.6 cm). This discrepancy between the two datasets is most likely related to the larger footprint size of Envisat radar altimeter and to its higher sensitivity of sea-ice properties. This result will be further discussed in the following section.

Surprisingly, the elevation of Envisat leads is found above the average elevation of sea-ice floes, which causes the radar free-
5 board to be negative (Fig. 3-d). In the literature, this phenomenon is attributed to the large difference between leads and ice floes waveform echoes (Laxon, 1994; Giles et al., 2008; Laxon et al., 2013). This effect was also observed when comparing sea level observations obtained over flat leads and over rough open ocean (Giles et al., 2012).

As surface roughness and snow volume scattering increase, radar waveform echoes become more diffuse. As threshold retrackers do not take into account the modification of the waveform shape, this phenomenon drive a bias on the range retrieval. More
10 specifically, altimetric ranges estimated with relatively specular echoes appear shorter than altimetric ranges estimated with diffuse echoes.

Unlike for Envisat, the average elevation of CryoSat-2 sea-ice floes is found above the sea level. As already shown in the study by Ricker et al. (2014), this result suggests that CryoSat-2 allows to retrieve realistic freeboard estimates with the use of a single retracker and without applying any constant correction. As suggested in the previous section, this difference between the
15 two sensors is mainly related to the difference of altimetric mode (SAR and pulse-limited). In SAR altimetry, the Doppler postprocessing allows to sharpen the surface response and minimize the sensitivity of the waveform shape to surface roughness and volume scattering (Raney, 1998). Consequently, SAR altimerty is less impacted by the variability of ice surface properties than pulse-limited altimetry, which enables to retrieve realistic (positive) freeboard estimates.

In most studies, the bias related to the difference of specularity is artificially corrected by applying a different retracking algo-
20 rithm to leads and ice floes and/or by applying an empirical constant correction (Giles et al., 2008; Laxon et al., 2013). As we seek to fully understand the impact of ice surface properties on CryoSat-2 and Envisat freeboard retrievals, we do not apply such correction at this stage of the freeboard retrieval.

3.3 Comparison of gridded radar freeboard estimates

25 As mentioned in the previous section, the difference of surface properties between leads and ice floes is generally expected to drive a constant bias on the freeboard estimates. In addition to this constant bias, the study by Kurtz et al. (2014) demonstrates that the variability of surface properties within ice floes (especially roughness variability) also drives a variable bias on the freeboard estimates when using a threshold retracking algorithm. Based on this result, we seek to analyse more in details the impact of sea-ice surface properties on CryoSat-2 and Envisat radar freeboard estimates.

30 As the along-track observations do not allow to compare strictly the same region, we now compare monthly gridded freeboard datasets. In Fig. 4a, we show monthly maps of the radar freeboard difference (Δfb) for the 2010/2011 ice growth season between Envisat and CryoSat-2 (Envisat - CryoSat-2).

For every Arctic regions and for each month of the period of study, CryoSat-2 is always thicker than Envisat (Δfb <0). This result is mostly due to the unrealistic negative Envisat freeboard estimates described in the previous section.

During the entire ice growth season, high Δfb observations are located over FYI in marginal regions as in the Bering Strait, at north of the Atlantic Ocean and in coastal regions. High Δfb are also particularly present at the beginning of the ice growth season. Conversely, low Δfb observations are mainly located over MYI areas at North Canadian Archipelago and are mostly visible at the end of winter. The evolution of the Δfb all along the winter season as well as its spatial distribution suggest that

5 the discrepancy between CryoSat-2 and Envisat radar freeboard estimates is related with the ice surface properties. In particular, variations of waveform shape driven by changes in ice roughness and snow accumulation are likely to be responsible for the observed variations of Δfb.

To further analyse the link between the variability of the ice surface properties and the radar freeboard discrepancy between Envisat and CryoSat-2, the waveform pulse-peakiness (PP) can be analysed. For Nadir-looking radar altimeters as Envisat and

10 CryoSat-2, high values of PP indicate the presence of flat and specular FYI while low values of PP indicate the presence of rough and snow covered MYI (Zygmuntowska et al., 2013). This phenomenon is also visible on the waveform echoes shown in Fig. 2.

In Fig. 4b, we show monthly maps of Envisat PP for the 2010/11 ice growth season. To build these maps, PP observations corresponding to leads have been removed. In November, most Arctic regions display a PP larger than 0.1. These relatively

15 high values are mainly explained by the presence of specular young sea-ice. Only rough MYI areas display PP observations lower than 0.1 during this period of the year. The average Envisat PP decreases progressively from 0.14 in November to 0.07 in April due to the ice growth, ice deformation and snow thickening that increase the ice surface diffusion. Only coastal regions keep displaying relatively high values of PP during the entire ice growth season.

Considering Fig. 4a and 4b, it is striking how the PP and the Δfb maps are correlated. This relation between the two parameters

20 is particularly visible in marginal and coastal regions where the PP and the Δfb are both relatively high.

To further demonstrate the link between the PP and the Δfb, we show in Fig. 5 the relation between the Δfb and the Envisat PP for November 2010-April 2011 (blue) and November 2011-March 2012 (red) as well as the polynomial regression obtained with the entire set of observation (dark dashed line). As suggested by the visual observations of Fig. 4, there is a clear correlation between the PP and the Δfb (R = 0.82). The radar freeboard difference varies from -33 cm for low PP to -18 cm for high

25 PP. Between the two ice growth seasons, the relation between the PP and the Δfb is fairly similar despite a slight discrepancy for low PP values (<0.08). The relatively high dispersion observed for low PP values between the two winter seasons is mostly driven by an insufficient sampling of thick freeboard/low PP estimates due to the relatively low amount of thick ice bellow 81.5°N during the period of study.

The linkage between the PP and the Δfb shown in Fig. 4 and Fig. 5 demonstrates that the discrepancy of radar freeboard

30 between CryoSat-2 and Envisat is related with the impact of surface properties on the radar signal. Considering that CryoSat-2 provides relatively accurate freeboard estimates and that SAR waveforms are less sensitive to ice surface properties, the linkage between the Δfb and the Envisat PP is most likely driven by a higher impact of ice surface properties on pulse-limited altimetry. This result is nothing more than an extension of the conclusions made in the previous section: Envisat waveform echoes are more impacted by the variability of ice surface properties than SAR waveform echoes (see Fig. 2). The higher sensitivity of

35 pulse-limited waveforms to ice surface properties tends to drive a variable bias on the altimetric range and thus on the freeboard

estimates. In particular, Fig. 5 suggests that Envisat radar freeboard is more underestimated over ice characterized by a low PP than over ice characterized by a high PP. In other words, the freeboard height is underestimated over thick and rough sea-ice and/or underestimated over thin and specular sea-ice. This finding is similar to the results shown in the study by Schwegmann et al. (2015).

3.4 Toward an improved Envisat freeboard: Envisat/PP

Sections 3.2 an 3.3 show that the current Envisat freeboard estimates should be corrected from 1) the constant elevation bias existing between leads and ice floes and 2) from the variable bias caused by the variability of ice surface properties (surface roughness and volume scattering) found within ice floes. While 1) can be reduced by using an empirical correction as operated in previous studies (Giles et al., 2008; Laxon et al., 2013), 2) requires a more sophisticated methodology.

A first approach could consist in developing a retracking algorithm model that takes into account the variability of ice surface properties as operated in Kurtz et al. (2014) instead of using threshold retrackers. While such model could provide accurate measurement of sea-ice freeboard, it requires accurate knowledge on sea-ice characteristics such as mean surface slope (diffusion), angular backscattering efficiency (specularity) and snow volume scattering properties, which are currently hardly measurable parameters.

Another approach to improve the Envisat freeboard retrievals would consist in correcting the Envisat radar freeboard from both 1) and 2) with the results obtained in the present study. In particular, the regression function y(PP) shown in Fig. 5 can be used to build a CryoSat-2-like version of Envisat freeboard, which should considerably improve the current estimates. Following this approach, we show in Fig. 6c the Envisat freeboard corrected as follows:

$$fb_{pp} = fb - y(PP) \tag{6}$$

Where fb_{pp} is the corrected Envisat radar freeboard (hereafter Envisat/PP), PP is the Envisat pulse-peakiness, fb is the un-corrected Envisat radar freeboard and and $y(PP)$ is the average relationship between PP and Δfb shown in black in Fig. 6.

Unlike for Envisat (Fig. 6a), the Envisat/PP dataset displays realistic positive freeboard estimates during the entire winter. Considering Fig. 6b and 6c, the Envisat/PP radar freeboard is very similar to the results obtained with CryoSat-2, with thick freeboard estimates over MYI and thinner estimates over FYI. As shown in Tab. 1, the RMSD between Envisat/PP and CryoSat-2 ($\sim$1.5 cm) is clearly better than the average RMSD between Envisat and CryoSat-2 ($\sim$23 cm).

To further assess the capacity of the PP-correction to provide a CryoSat-2-like version of Envisat freeboard, we show in Fig. 6d the Probability Distribution Function (PDF) of the Envisat/PP (blue) and CryoSat-2 (black) radar freeboard estimates. We also provide the average bias and average Root Mean Square Difference between the two datasets in Tab. 1. For each month of the period of study, the distribution of the Envisat/PP and CryoSat-2 datasets are relatively similar with quasi-identical mean and modal values. Only November and in a lesser extent December, show a discrepancy between the two datasets with an

overestimation of Envisat radar freeboard estimates. This result could be due to a lower accuracy of the native Envisat radar freeboard estimates and/or to a lower performance of the PP-correction during this period for which the amount of specular scattering is relatively high.

In addition to the spatial variability, the Envisat/PP and CryoSat-2 datasets display relatively similar seasonal variations with an increase of respectively 3.4 cm and 2.1 cm between November 2010 and April 2011 and of 3.0 cm and 3.3 cm between November 2011 and March 2012 (see Tab. 1). This result suggests that unlike for the native Envisat radar freeboard estimates (Kern et al., 2015), the Envisat/PP should allow to derive a realistic seasonal ice growth cycle.

The relatively good match between CryoSat-2 and Envisat/PP radar freeboard demonstrates that the PP correction allows to build a robust CryoSat-2-like version of Envisat freeboard during each month of the common flight period of Envisat and CryoSat-2 missions.

3.5 Comparison to BGEP ice draft measurements

To assess the potential of the PP-correction approach to produce accurate ice thickness estimates, we now convert the CryoSat-2, Envisat and Envisat/PP radar freeboard datasets to sea-ice draft (thickness - freeboard) fields and compare the results to BGEP ice draft measurements. For this purpose, we estimate the monthly median altimetric ice draft within a radius of 50 km around each available mooring, which we compare to the corresponding monthly median mooring ice draft.

In Fig. 7, we show the monthly CryoSat-2 and Envisat/PP ice draft estimates as a function of the corresponding monthly BGEP ice draft. In color, we represent the MYI fraction for each observation. We also provide in Tab. 2, statistical parameters (mean bias, RMSE and correlation coefficient) for each dataset.

CryoSat-2 ice draft estimates display a relatively low RMSE (15 cm) with *in situ* measurements during the 2010/11 ice growth season (Fig. 7a) and a higher RMSE (21 cm) during the 2011/12 ice growth season (Fig. 7b). The higher RMSE observed in Fig. 7b is mainly driven by a few values characterized by a low MYI fraction. This result suggests that the higher RMSE obtained during 2011/12 might be caused by an inaccurate snow depth and/or ice density parametrizations rather than by an error in the freeboard fields.

The comparison of the Envisat/PP and Envisat datasets during the 2010/12 period clearly shows the improvement brought by the PP-correction (see Tab. 2). The lower mean bias and RMSE is mostly due to the correction of the average bias between leads and ice floes (further up identified as "1)") while the improved correlation coefficient is mostly due to the correction of the variable bias existing within ice floes (further up identified as "2)").

The correlation between the Envisat/PP dataset and the BGEP ice draft measurements displays a low RMSE (12 cm) during winter 2010/11 (Fig. 7j) and a relatively higher RMSE (28 cm) during winter 2011/12 (Fig. 7k). As for CryoSat-2, we attribute this difference to a potential inaccurate freeboard-to-thickness conversion.

To further assess the potential of the PP correction, it is necessary to verify if the Envisat/PP dataset is also valid out of the cross-calibration period. As the BGEP ice draft measurements are available from August 2003, the accuracy of the PP-correction can be evaluated over most of the Envisat mission lifetime. The Envisat and Envisat/PP ice draft estimates are therefore computed over the 2003-2010 ice growth seasons and are compared with the corresponding mooring observations. Results are presented

in Tab. 2 and in Fig. 7c-i.

As during the 2010-2012 period, the Envisat/PP ice draft dataset displays a good agreement with the buoys observations (RMSE = 13 to 32 cm) relatively to the uncorrected Envisat dataset (RMSE = 165 to 186 cm). This good agreement between the Envisat/PP and the BGEP ice draft estimates demonstrates therefore that the Envisat/PP dataset provides accurate estimates

5   of sea-ice draft during the entire Envisat mission.

The largest improvements brought by the PP correction are particularly visible for winter seasons occurring right after low sea-ice summer extent (2007/08, 2008/09, 2010/11 and 2011/12). As displayed in Fig. 7, these winter seasons are characterized by mixed FYI and MYI and thus by heterogeneous sea ice conditions (surface roughness, snow depth, etc). This result confirms therefore that the PP-corrections allows to reduce the impact of ice properties on the freeboard estimates and that it enables to

10   retrieve more accurate ice thickness estimates.

4   Discussion

In section 3.1, we show that the variability of ice surface properties has a stronger impact on Envisat waveforms than on CryoSat-2 waveforms (especially between FYI and MYI). Based on this observation, we conclude that CryoSat-2 radar free-board should provide with relatively accurate estimates of radar freeboard relatively to Envisat. Nevertheless, one can still

15   observe a variability of CryoSat-2 waveform echoes depending on the ice type. This result suggests that while the sensitivity of CryoSat-2 waveforms is relatively low, the radar freeboard derived from CryoSat-2 is also likely to be biased by the ice surface properties. In the study by Kurtz et al. (2014), the authors demonstrate that the variability of the ice surface properties between ice floes (mainly ice roughness) drives a bias in CryoSat-2 freeboard estimates when using a threshold retracker. Having said that, the comparison of our CryoSat-2 ice draft estimates with *in situ* measurements as well as preliminary studies

20   (Laxon et al., 2013; Kwok and Cunningham, 2015; Tilling et al., 2015) demonstrate that CryoSat-2 freeboard estimates are fairly accurate despite the use of a threshold retracker. Consequently, the impact of CryoSat-2 freeboard uncertainty on the Envisat/PP estimates should be minor. The exercise operated in the present study could nevertheless be repeated with better CryoSat-2 estimates to derive a more accurate PP-correction, which could further improve the Envisat freeboard estimates.

While the PP-correction allows to remove most of the bias between CryoSat-2 and Envisat freeboard datasets, other sources of

25   inconsistencies could explain the remaining difference between the 2 datasets. For instance, bright off-nadir reflexions have a higher impact on Envisat than on CryoSat-2. The reduced footprint of CryoSat-2 allows to filter out bright off-nadir reflections in the along-track direction, which enables to produce more accurate estimates of surface level position than with Envisat. As this discrepancy between the two radar altimeters is not corrected by the PP-correction, the Envisat/PP freeboard is therefore likely less accurate than CryoSat-2's. Another source of discrepancy between SAR and pulse-limited altimetry is the size of

30   the sampled ice floes. Thanks to the Doppler post-processing, the SAR mode of CryoSat-2 allows to sample smaller ice floes than Envisat. As small ice floes are generally thinner than large ice floes, this difference could drive a sampling bias between the two sensors. More specifically, Envisat freeboard is likely to overestimate regional freeboard height. The only thing one

can do to reduce this sampling bias would be to estimate freeboard height when sea-ice is as compact as possible (in the middle of winter for example).

5 Conclusions

In this study we investigate on the inconsistency between CryoSat-2 and Envisat radar freeboard estimates during the common
5 flight period (November 2010-April 2011 and November 2011-March 2012). The analysis of the along-track surface elevation estimates shows that the average Envisat ice floes elevation is always found bellow the sea level. This unrealistic result is attributed to the high difference of waveform shape acquired over specular and diffuse surfaces and to the use of a threshold retracker. Unlike Envisat, the average CryoSat-2 elevation of ice floes is mostly found above the sea level, which allows to retrieve realistic freeboard estimates. The better results of CryoSat-2 are attributed to the SAR post-processing that allows to
10 sharpen the radar response and reduces the impact of ice surface properties on waveform echoes.

The analysis of the gridded freeboard height difference between CryoSat-2 and Envisat shows that the discrepancy between the two sensors is larger over over ice characterized by a low PP than over specular and young ice characterized by a high PP. Here as well, this discrepancy is attributed to the higher sensitivity of Envisat waveform echoes to sea-ice surface properties (surface roughness and snow volume scattering).

15 While the average difference of waveform shape between leads and ice floes is generally corrected by the use of a different retracking algorithm for leads and ice floes in freeboard retrieval processings, the bias due to the variability of sea-ice surface properties has yet never been taken into account in Envisat freeboard studies. To correct these 2 biases, we build an improved Envisat freeboard dataset (Envisat/PP) based on the relation between the freeboard difference between Envisat and CryoSat-2 and the Envisat PP. The resulting Envisat/PP freeboard estimates displays similar patterns as CryoSat-2 during the entire
20 period of study (RMSD = $\sim$ 1.5 cm) and offers a more realistic seasonal cycle ($\sim$ 2.0 to 3.0 cm) than the uncorrected Envisat freeboard.

The comparison of each altimetric dataset with *in situ* ice draft observations during the common flight period reveals that Envisat/PP ice draft is highly more accurate (RMSE = 12 - 28 cm) than the uncorrected Envisat dataset (RMSE = 178 - 179 cm) and as accurate as CryoSat-2 (RMSE = 15 - 21 m).

25 To further assess the potential of the PP-correction, the Envisat and Envisat/PP ice draft datasets are extended to the 2003-2010 period and are similarly compared to BGEP ice draft measurements. As for the 2010-2012 period, the agreement with *in situ* measurements is higher for Envisat/PP (RMSE = 13 - 32 cm) than for Envisat (RMSE = 165 - 186 cm), which demonstrates the potential of the PP-correction to provide accurate freeboard estimates over the entire Envisat mission lifetime.

The result obtained in the present study should therefore allow to derive circumpolar sea-ice thickness over more than a decade
30 by combining Envisat and CryoSat-2 datasets and should help to improve our understanding of the undergoing Arctic sea ice changes.
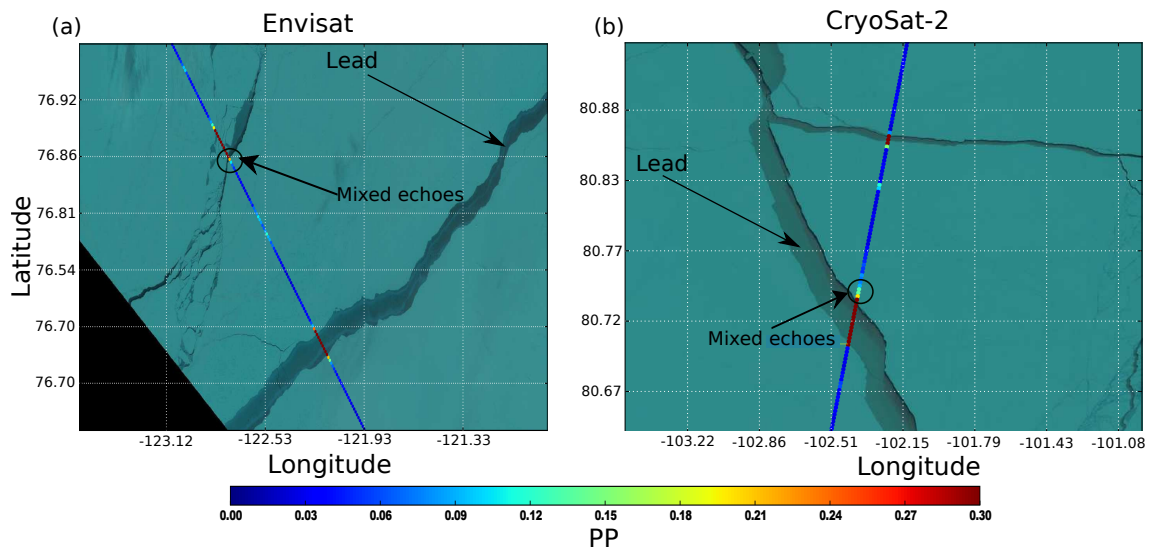
Figure 1. (a) PP spatial variability along Envisat track (16 April 2003) plotted over a Landsat-7 LandsatLook Image acquired on the same day and (b) PP spatial variability along CryoSat-2 track (01 May 2015) plotted over a Landsat-8 LandsatLook Image also acquired on the same day. For both figures, each dot represents a 20 Hz PP measurement.
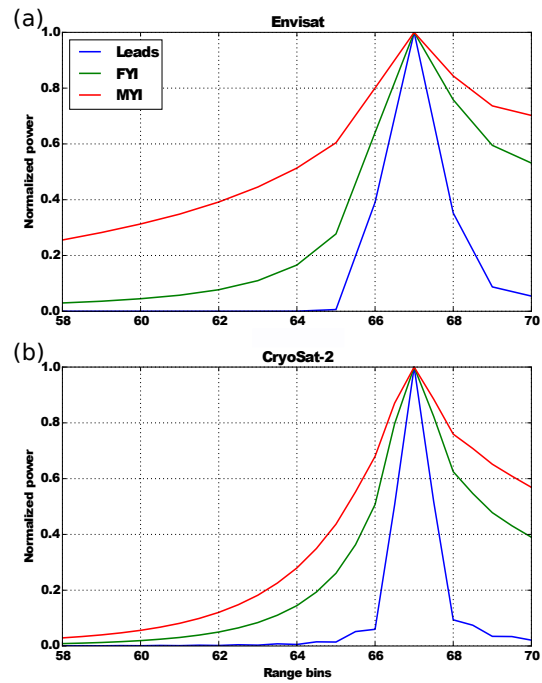
Figure 2. (a) Envisat and (b) CryoSat-2 mean waveform echoes for Leads (blue), FYI (green) and MYI (red) calculated during the 2010/11 winter and for the entire common flight region.
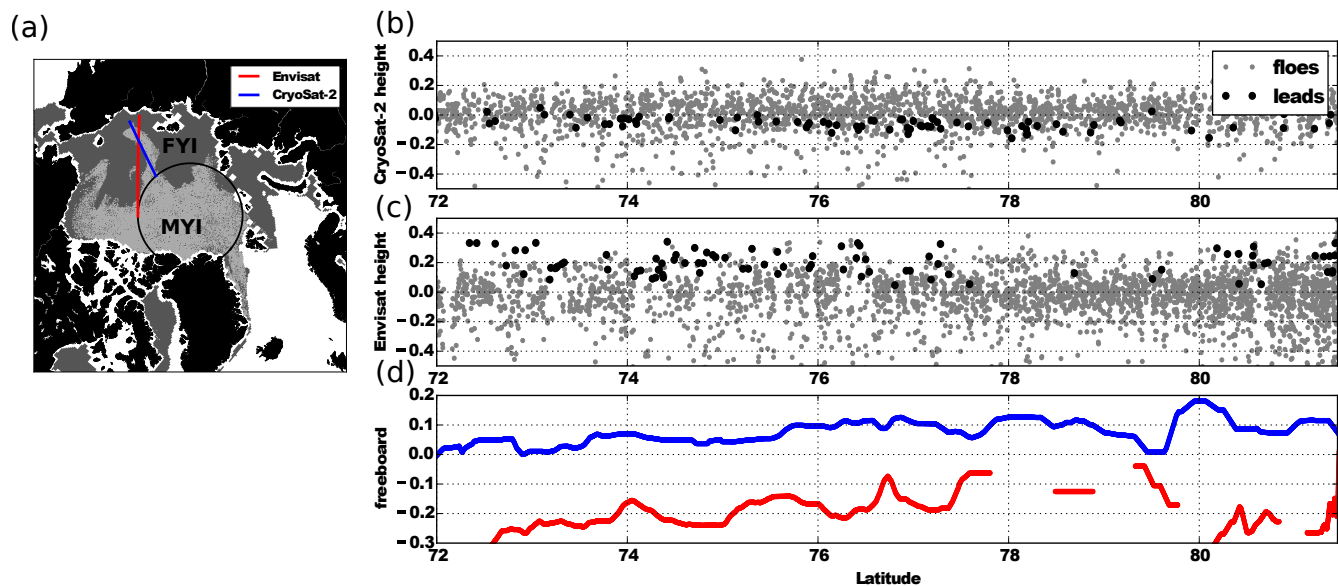
Figure 3. (a) Map of the Envisat (red) and CryoSat-2 (blue) tracks (both monitored on the 24 February 2011) selected for the along-track analysis of the radar freeboard. The light shading shows MYI regions (defined as sea ice with a MYI fraction above 0.7) and the dark gray shading shows FYI regions (defined as sea ice with a MYI bellow 0.7). (b) CryoSat-2 and (c) Envisat leads (gray dots) and ice floes (black dots) surface elevation corresponding to the tracks shown in (a). (d) Envisat (red) and CryoSat-2 (blue) freeboard corresponding to the tracks shown in (a).
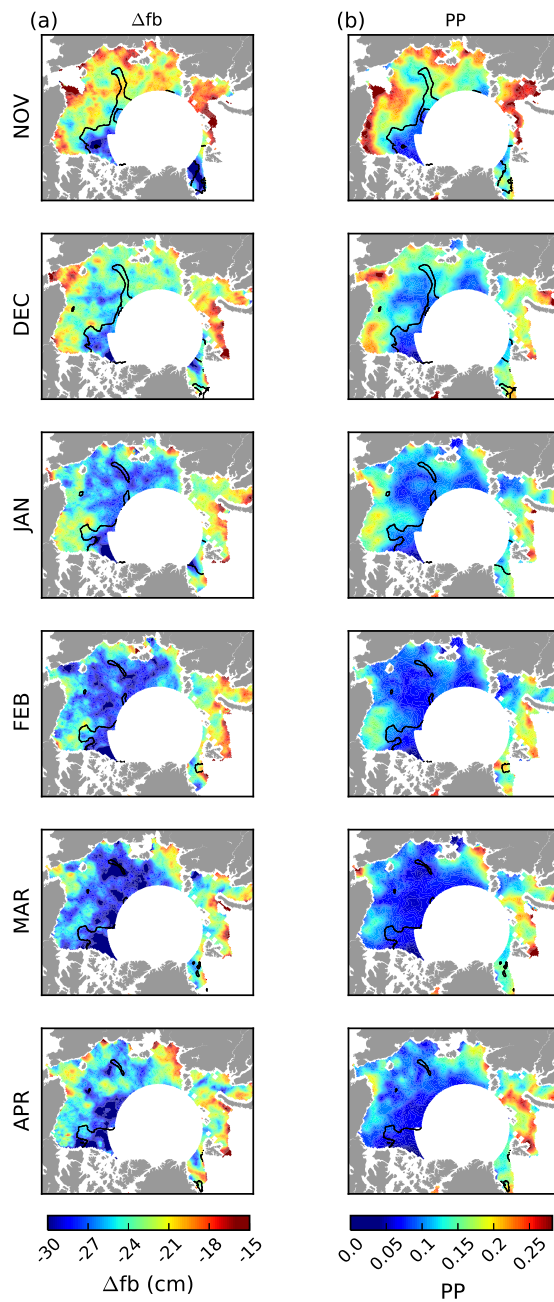
Figure 4. (a) Monthly freeboard difference (Δfb) between Envisat and CryoSat-2 and (b) monthly Envisat pulse peakiness (PP) shown for the November 2010 - March 2012 period. The dark lines represent the isoline MYI fraction equal to 0.7
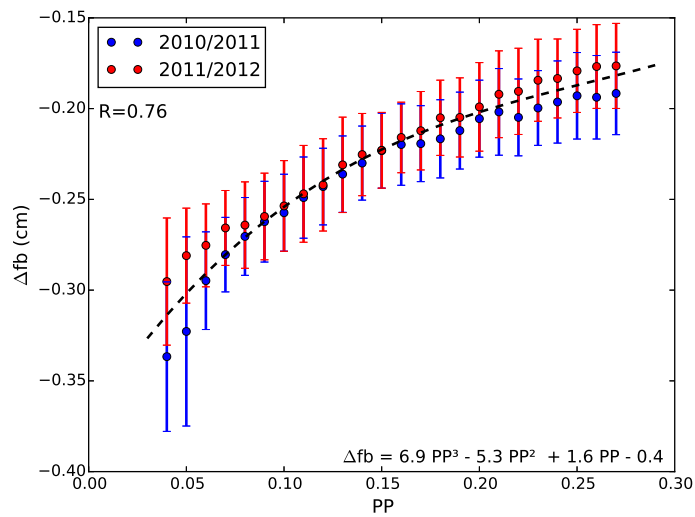
Figure 5. Relation between the monthly freeboard difference between Envisat and CryoSat-2 (Δfb) and the monthly Envisat pulse-peakiness (PP) shown for winter 2010/2011 (blue) and 2011/2012 (red). The error bars show the corresponding standard deviation for each value and the dark tilted line represents the linear fit of all monthly observations (November 2010 - April 2011 and November 2011 - March 2012). At the bottom of the figure we provide the linear function of the corresponding fit.
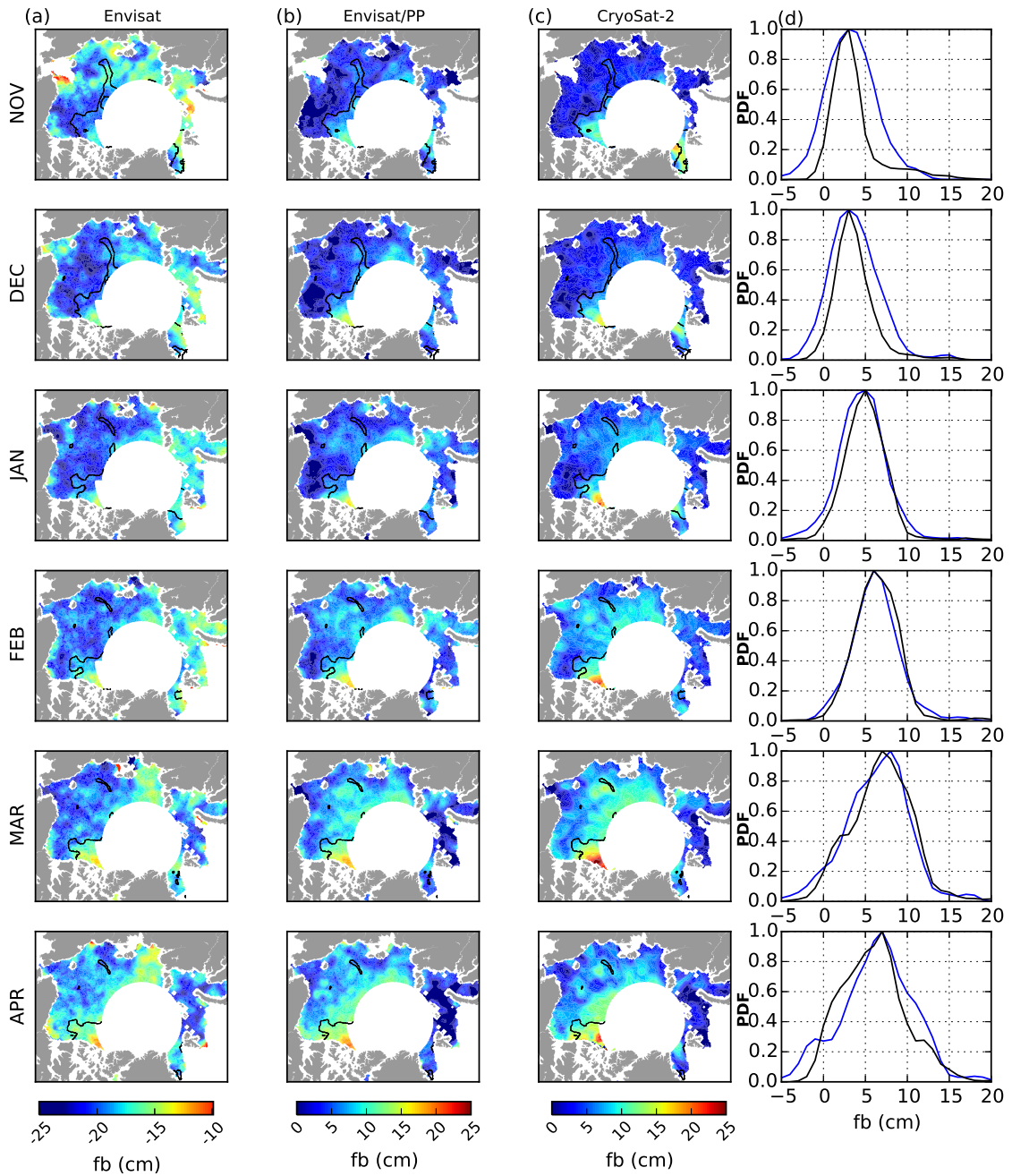
Figure 6. (a) Envisat, (b) Envisat/PP and (c) CryoSat-2 monthly freeboard maps shown for the November 2010 - April 2011 period. The dark lines represent the isoline fraction of MYI equal to 0.7. (d) Probability Distribution Function (PDF) of Envisat (blue) and CryoSat-2 (black) radar freeboard.
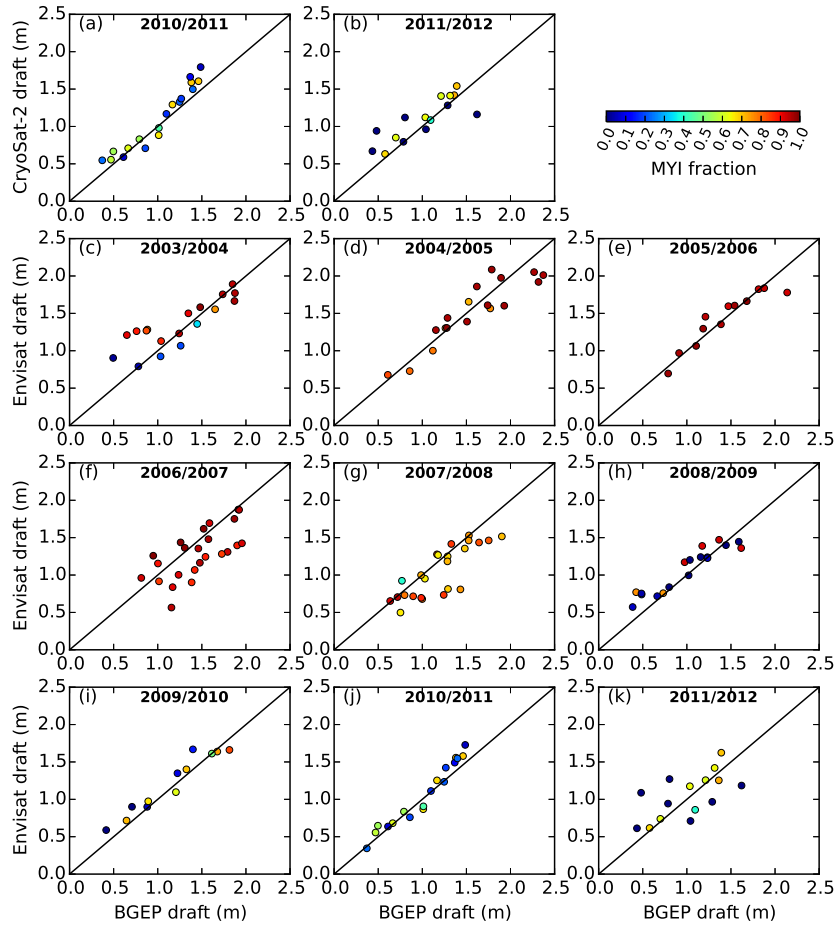
Figure 7. CryoSat-2 monthly ice draft as a function of BGEP moorings monthly median ice draft for winters 2010/11 (a) and 2011/12 (b). Envisat/PP monthly ice draft as a function of BGEP moorings monthly median ice draft for winters 2003/04 to 2011/12 (c-k). The colormap shows the corresponding Multi Year Ice (MYI) fraction.

Table 1. Monthly mean Envisat, Envisat/PP and CryoSat-2 circumpolar radar freeboard estimates and monthly mean circumpolar RMSD between Envisat and CryoSAt-2 and between Envisat/PP and CryoSat-2.

	Envisat mean	Envisat/PP mean	CryoSat-2 mean	Envisat-CryoSat-2 RMSD	Envisat/PP-CryoSat-2 RMSD
2010/11					
NOV	-18.1	3.2	3.0	21.3	1.4
DEC	-19.2	3.5	3.3	23.1	1.3
JAN	-19.3	4.6	4.9	24.7	1.6
FEB	-18.6	6.2	6.3	25.6	1.6
MAR	-18.8	6.6	7.1	26.2	1.5
APR	-18.2	6.6	6.0	24.6	1.5
2011/12					
NOV	-16.9	4.2	3.0	19.7	1.8
DEC	-18.1	4.3	3.4	21.8	1.5
JAN	-18.7	5.8	6.1	24.1	1.3
FEB	-19.2	5.8	6.1	25.6	1.7
MAR	-18.3	6.3	6.3	25.1	1.6

Table 2. Average winter bias, Root Mean Square Error (RMSE) and correlation coefficient (R) between the altimetric and BGEP ice draft estimated during winters 20003/04 to 2011/12 for Envisat and during winters 2010/11 and 2011/12 for CryoSat-2.

	Envisat		Envisat/PP		CryoSat-2	
	bias (RMSE)	R	bias (RMSE)	R	bias (RMSE)	R
2003/04	-134 (165)	0.84	10 (26)	0.84	-	-
2004/05	-170 (172)	0.91	-5 (21)	0.90	-	-
2005/06	-170 (170)	0.90	0 (14)	0.93	-	-
2006/07	-174 (175)	0.86	-17 (31)	0.69	-	-
2007/08	-165 (167)	0.70	-15 (25)	0.81	-	-
2008/09	-183 (186)	0.56	8 (17)	0.94	-	-
2009/10	-184 (186)	0.89	6 (13)	0.96	-	-
2010/11	-178 (179)	0.78	6 (12)	0.97	9 (15)	0.96
2011/12	-174 (178)	0.34	4 (28)	0.63	10 (21)	0.82

Acknowledgements. This research is supported by the French CNES TOSCA SICKAyS. We thank the Center for Topographic studies of the Oceans and Hydrosphere (CTOH) at LEGOS for providing the SGDR Envisat and CryoSat-2 data.

References

Alexandrov, V., Sandven, S., Wahlin, J., and Johannessen, O.: The relation between sea ice thickness and freeboard in the Arctic, The Cryosphere, 4, 373–380, 2010.

5   Andersen, O. B., G. P. L. S. and Knudsen, P.: The DTU15 Mean Sea Surface and Mean Dynamic Topography- focusing on Arctic issues and development,, in: oral presentation, in the 2015 OSTST Meeting , Reston, USA., 2015.

Anderson, M., A. C. B. and Tschudi, M.: MEaSUREs Arctic Sea Ice Characterization Daily 25km EASE-Grid 2.0, Version 1. Boulder, Colorado USA. NASA National Snow and Ice Data Center Distributed Active Archive Center., doi:http://dx.doi.org/10.5067/MEASURES/CRYOSPHERE/nsidc-0532.001, 2014.

10   Beaven, S. G.: Sea Ice Radar Backscatter Modeling, Measurements, and the Fusion of Active and Passive Microwave Data., Tech. rep., DTIC Document, 1995.

Carrere, L., Lyard, F., Cancet, M., and Guillot, A.: FES 2014, a new tidal model on the global ocean with enhanced accuracy in shallow seas and in the Arctic region, in: EGU General Assembly Conference Abstracts, vol. 17, p. 5481, 2015.

Chelton, D. B., Ries, J. C., Haines, B. J., Fu, L.-L., and Callahan, P. S.: Satellite altimetry, International geophysics, 69, 1–ii, 2001.

15   Comiso, J. C.: Large Decadal Decline of the Arctic Multiyear Ice Cover, Journal of Climate, 25, 1176–1193, 2012.

Connor, L. N., Laxon, S. W., Ridout, A. L., Krabill, W. B., and McAdoo, D. C.: Comparison of Envisat radar and airborne laser altimeter measurements over Arctic sea ice, Remote Sensing of Environment, 113, 563–570, 2009.

Giles, K. A., Laxon, S. W., and Ridout, A. L.: Circumpolar thinning of Arctic sea ice following the 2007 record ice extent minimum, Geophysical Research Letters, 35, 2008.

20   Giles, K. A., Laxon, S. W., Ridout, A. L., Wingham, D. J., and Bacon, S.: Western Arctic Ocean freshwater storage increased by wind-driven spin-up of the Beaufort Gyre, Nature Geoscience, 5, 194–197, 2012.

Guerreiro, K., Fleury, S., Zakharova, E., Rémy, F., and Kouraev, A.: Potential for estimation of snow depth on Arctic sea ice from CryoSat-2 and SARAL/AltiKa missions, Remote Sensing of Environment, 186, 339–349, 2016.

Helm, V., Humbert, A., and Miller, H.: Elevation and elevation change of Greenland and Antarctica derived from CryoSat-2, The Cryosphere, 25   8, 1539–1559, 2014.

Holloway, G. and Sou, T.: Has Arctic Sea Ice Rapidly Thinned?, Journal of Climate, 15, 1691–1701, doi:10.1175/1520-0442(2002)015<1691:HASIRT>2.0.CO;2, 2002.

Kern, S., Khvorostovsky, K., Skourup, H., Rinne, E., Parsakhoo, Z., Djepa, V., Wadhams, P., and Sandven, S.: The impact of snow depth, snow density and ice density on sea ice thickness retrieval from satellite radar altimetry: results from the ESA-CCI Sea Ice ECV Project 30   Round Robin Exercise, The Cryosphere, 9, 37–52, 2015.

Kurtz, N., Farrell, S., Studinger, M., Galin, N., Harbeck, J., Lindsay, R., Onana, V., Panzer, B., and Sonntag, J.: Sea ice thickness, freeboard, and snow depth products from Operation IceBridge airborne data, 2013.

Kurtz, N. T., Galin, N., and Studinger, M.: An improved CryoSat-2 sea ice freeboard retrieval algorithm through the use of waveform fitting, 2014.

35   Kwok, R.: Annual cycles of multiyear sea ice coverage of the Arctic Ocean: 1999–2003, Journal of Geophysical Research: Oceans, 109, 2004.

Kwok, R. and Cunningham, G.: Variability of Arctic sea ice thickness and volume from CryoSat-2, Phil. Trans. R. Soc. A, 373, 20140 157, 2015.

Kwok, R. and Rothrock, D.: Decline in Arctic sea ice thickness from submarine and ICESat records: 1958–2008, Geophysical Research Letters, 36, 2009.

Laxon, S.: Sea ice altimeter processing scheme at the EODC, International Journal of Remote Sensing, 15, 915–924, 1994.

5   Laxon, S., Peacock, N., and Smith, D.: High interannual variability of sea ice thickness in the Arctic region, Nature, 425, 947–950, 2003.

Laxon, S. W., Giles, K. A., Ridout, A. L., Wingham, D. J., Willatt, R., Cullen, R., Kwok, R., Schweiger, A., Zhang, J., Haas, C., et al.: CryoSat-2 estimates of Arctic sea ice thickness and volume, Geophysical Research Letters, 40, 732–737, 2013.

Peacock, N. R. and Laxon, S. W.: Sea surface height determination in the Arctic Ocean from ERS altimetry, Journal of Geophysical Research: Oceans, 109, 2004.

10 Raney, R. K.: A delay/Doppler radar altimeter for ice sheet monitoring, in: Geoscience and Remote Sensing Symposium, 1995. IGARSS '95. 'Quantitative Remote Sensing for Science and Applications', International, vol. 2, pp. 862–864 vol.2, doi:10.1109/IGARSS.1995.521080, 1995.

Raney, R. K.: The delay/Doppler radar altimeter, IEEE Transactions on Geoscience and Remote Sensing, 36, 1578–1588, 1998.

Ricker, R., Hendricks, S., Helm, V., Skourup, H., and Davidson, M.: Sensitivity of CryoSat-2 Arctic sea-ice freeboard and thickness on
15 radar-waveform interpretation, The Cryosphere, 8, 1607–1622, 2014.

Ridout, A., N. I. and Tonboe., R. T.: Sea Ice Climate Change Initiative: Phase 1 . European Space Agency, SICCI-ATBDv0-07-12,, 2012.

Rothrock, D. A., Yu, Y., and Maykut, G. A.: Thinning of the Arctic sea-ice cover, Geophysical Research Letters, 26, 3469–3472, 1999.

Schwegmann, S., Rinne, E., Ricker, R., Hendricks, S., and Helm, V.: About the consistency between Envisat and CryoSat-2 radar freeboard retrieval over Antarctic sea ice, The Cryosphere Discuss., 9, 4893-4923, doi: 10.5194/tcd-9-4893, 2015.

20 Tilling, R. L., Ridout, A., Shepherd, A., and Wingham, D. J.: Increased Arctic sea ice volume after anomalously low melting in 2013, Nature Geoscience, 8, 643–646, 2015.

Warren, S. G., Rigor, I. G., Untersteiner, N., Radionov, V. F., Bryazgin, N. N., Aleksandrov, Y. I., and Colony, R.: Snow depth on Arctic sea ice, Journal of Climate, 12, 1814–1829, 1999.

Wingham, D., Francis, C., Baker, S., Bouzinac, C., Brockley, D., Cullen, R., de Chateau-Thierry, P., Laxon, S., Mallow, U., Mavrocordatos,
25 C., et al.: CryoSat: A mission to determine the fluctuations in Earth's land and marine ice fields, Advances in Space Research, 37, 841–871, 2006.

Zygmuntowska, M., Khvorostovsky, K., Helm, V., and Sandven, S.: Waveform classification of airborne synthetic aperture radar altimeter
510 over Arctic sea ice, Arctic sea ice altimetry-advances and current uncertainties, 2013.